

Diffraction of Weakly Bound Clusters: Spectroscopy and Size Effects*

Martin Stoll[†], Thorsten Köhler[‡] and Gerhard C. Hegerfeldt[†]

February 9, 2020

Abstract

Exciting experiments in the field of atom and molecule optics have lately drawn much attention to the effects involved in the coherent diffraction of particle beams. We review the influence of the finite size of the particles and of their energy level spectrum on the diffraction pattern. In turn, we demonstrate how experimental diffraction measurements allow to determine these quantities of weakly bound molecules by considering the diffraction of $^4\text{He}_2$, $^4\text{He}_3$, and $(\text{D}_2)_2$.

1 Introduction

As early as 1927 the wave-like properties of matter were demonstrated when an electron beam was diffracted by a crystal of nickel [1]. Recently, propelled by the availability of custom-made nano-structured transmission gratings with periods as small as 100 nm, typical diffraction experiments from light optics have been carried over to the domain of atom and molecule optics [2, 3, 4, 5]. Nowadays, these experiments serve as precision measurement devices for, e.g., the interaction of atoms and molecules with solid surfaces [6, 7] or as quantum mechanical mass spectrometers [8, 9].

Owing to the great sensitivity of these experiments it was soon realized that a semi-classical theory using de Broglie waves and the results from light optics otherwise does not yield an accurate explanation of the experimental observations [6, 9]. Only by a fully quantum mechanical approach, based on few-body scattering theory, could the diffraction pattern of a collimated beam of helium atoms and helium clusters be described [10, 11]. Since all particles in such a beam share the same (average) velocity their de Broglie wave lengths are inversely proportional to their masses. Therefore, their diffraction angles are scaled by the same factor. On the one hand this mass-selective property allowed to ascribe certain experimental diffraction maxima to heavy clusters up to $^4\text{He}_{26}$ [12]. On the other hand the diffraction of the diatomic helium cluster (“dimer”) could be quantitatively studied and its bond length and binding energy could be determined [9].

*Invited talk given at the TH2002 International Conference on Theoretical Physics, Paris, July 22-27 2002

[†]Institut für Theoretische Physik, Universität Göttingen

[‡]Clarendon Laboratory, Department of Physics, University of Oxford

Moreover, atoms or molecules may coherently undergo internal transitions upon interaction with the diffracting object. Inelastic diffraction from a transmission grating involving transitions of metastable argon atoms [13] and nitrogen dimers [14] has already been observed. In these experiments, however, the grating served only to increase the intensity diffracted by the slits. In the case of coherent diffraction from many slits of a grating, inelastic diffraction gives rise to separate additional diffraction maxima. The diffraction angles at which these new maxima appear are related to the transition energies in a characteristic way. This was first discussed for the particularly interesting case of the three-body cluster of helium (“trimer”) [15] in order to produce the predicted excited state, which is believed to be of Efimov-type (see, e. g., Ref. [16]). Recently, the theory of inelastic diffraction was also applied to the examples of the van der Waals dimers H_2D_2 and $(\text{D}_2)_2$ [17]. Their energy level spectra are well known [18]. Therefore, they may serve to compare the theory to experimental data.

2 Diffraction of very weakly bound molecules

In this section we will review some aspects of the theory of molecular diffraction. Our approach has been described in detail before [10, 11]. Therefore, we will focus on the final steps of the calculation which lead to the desired results. These results relate the experimentally recordable diffraction pattern to internal quantities of the molecular bound state: the energy level spectrum and the bond length. Only the experimentally most relevant case of diffraction from a nano-scale transmission grating will be considered.

We choose the coordinate system such that the z axis is parallel to the bars of the grating (cf. figure 1). As an idealization, we assume the grating to be

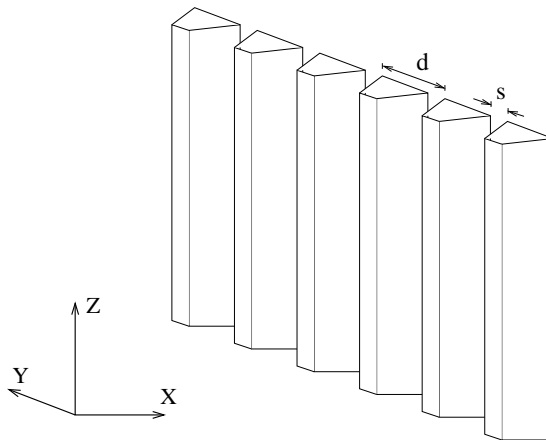


Figure 1: The coordinate system is chosen such that the bars of the transmission grating are parallel to the z axis, and that the grating is periodic in the y direction. The period is denoted by d , and the slit width by s .

translationally invariant along the z axis. Therefore, the z -component of the incident momentum is conserved, and the diffraction problem has effectively

been reduced to the xy plane. A typical transmission grating, as considered in this article, has a period of $d = 100$ nm and a slit width of $s \approx 70$ nm. The de Broglie wave length of a helium dimer at a velocity of 1 km/s, for example, is $\lambda_{\text{dB}} \approx 0.05$ nm. Therefore, the diffraction angles are of the order of several mrad about the forward direction.

The diffraction pattern of a well-collimated particle beam is, quite generally, determined by the transition amplitude between the incident and final momenta. For atoms, which are regarded as point-like particles (PP) here, of mass M with incident momentum \mathbf{P}' and final momentum $\mathbf{P} = \mathbf{P}' + \Delta\mathbf{P}$, the transition amplitude is given by [11]

$$t^{\text{PP}}(P_x, P_y; P'_x, P'_y) = -i \frac{P_x}{(2\pi)^2 M \hbar} \int dY \exp(-i\Delta P_y Y / \hbar) [1 - \tau^{\text{PP}}(P'_x, P'_y; Y)]. \quad (1)$$

Here, τ^{PP} is the transmission function characterizing the grating. In the special case where the grating bars are assumed to be purely repulsive, equation (1) recovers the well-known Kirchhoff diffraction amplitude from classical optics [19, chap. 8.5].

A corresponding result may be obtained for dimers. The masses of the constituents of a dimer are denoted by m_1 and m_2 , and the total mass is $M = m_1 + m_2$. The interaction between the constituents is accounted for by a two-body potential $V(\mathbf{r})$, where \mathbf{r} denotes the relative coordinate in the dimer. Bound dimer states supported by $V(\mathbf{r})$ are denoted by their wave functions $\phi_\gamma(\mathbf{r})$ with corresponding binding energies E_γ . In the following, we will always assume that the kinetic energy of an incident dimer exceeds the ground state energy E_0 of the dimer by far. This requirement is easily met for the cases considered in this article. For example, the kinetic energy of a helium dimer at a velocity of 1 km/s is of the order of 40 meV whereas the binding energy of its single bound state is $|E_0| \approx 0.1 \mu\text{eV}$ [9]. Hence upon diffraction from the grating, excitation as well as break-up of the dimer may occur. For an incident dimer in bound state $\phi_{\gamma'}$ with momentum \mathbf{P}' , the transition amplitude to the state ϕ_γ with final momentum $\mathbf{P} = \mathbf{P}' + \Delta\mathbf{P}$ is given by [11]

$$t(P_x, P_y, \phi_\gamma; P'_x, P'_y, \phi_{\gamma'}) = -i \frac{P_x}{(2\pi)^2 M \hbar} \int dY \exp(-i\Delta P_y Y / \hbar) [\delta_{\gamma\gamma'} - \tau_{\gamma\gamma'}^{\text{dim}}(P'_x, P'_y; Y)], \quad (2)$$

where the corresponding dimer transmission function is given as the weighted product of two point-particle transmission functions (cf. figure 2),

$$\tau_{\gamma\gamma'}^{\text{dim}}(P'_x, P'_y; Y) = \int d^3r \phi_\gamma^*(\mathbf{r}) \phi_{\gamma'}(\mathbf{r}) \times \tau_1^{\text{PP}} \left(\frac{m_1}{M} P'_x, \frac{m_1}{M} P'_y, Y + \frac{m_2}{M} y \right) \tau_2^{\text{PP}} \left(\frac{m_2}{M} P'_x, \frac{m_2}{M} P'_y, Y - \frac{m_1}{M} y \right). \quad (3)$$

Finally, under similar assumptions the transition amplitude for trimers may be derived. For simplicity, we specialize to the case where all three constituents have equal masses $m = M/3$, as in the helium trimer ${}^4\text{He}_3$. It can be shown that equation (2) also holds for trimers, if the dimer transmission function is

substituted by its trimer equivalent,

$$\begin{aligned} \tau_{\gamma\gamma'}^{\text{tri}}(P'_x, P'_y; Y) &= \int d^3r d^3\rho \phi_{\gamma}^*(\mathbf{r}, \boldsymbol{\rho}) \phi_{\gamma'}(\mathbf{r}, \boldsymbol{\rho}) \tau_1^{\text{PP}} \left(\frac{1}{3}P'_x, \frac{1}{3}P'_y; Y + \frac{2}{3}\rho_y \right) \\ &\times \tau_2^{\text{PP}} \left(\frac{1}{3}P'_x, \frac{1}{3}P'_y; Y - \frac{1}{3}\rho_y + \frac{1}{2}r_y \right) \tau_3^{\text{PP}} \left(\frac{1}{3}P'_x, \frac{1}{3}P'_y; Y - \frac{1}{3}\rho_y - \frac{1}{2}r_y \right). \end{aligned} \quad (4)$$

The Jacobi coordinates $(\mathbf{r}, \boldsymbol{\rho})$, and an interpretation of the position arguments involving r_y and ρ_y are shown in figure 2.

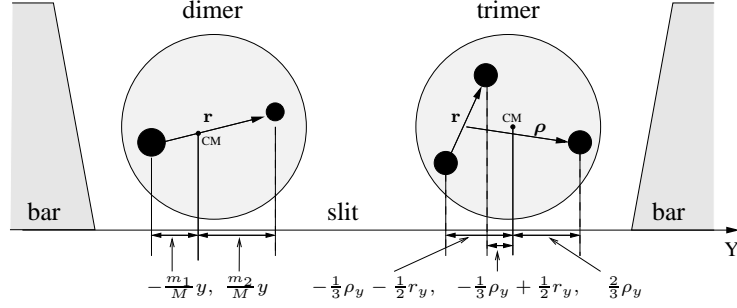


Figure 2: The position arguments of the functions τ_i^{PP} in equations (3) and (4) can be interpreted as projected displacements of the positions of the constituents of the dimer, or trimer, from the center of mass position Y .

Whereas the intensities of the diffraction maxima are given by the modulus square of the transition amplitude [11], two kinematic relations determine their angular positions. Firstly, energy conservation requires that

$$(P_x'^2 + P_y'^2)/2M + E_{\gamma'} = (P_x^2 + P_y^2)/2M + E_{\gamma} \quad (5)$$

(for the case of atom diffraction the binding energies $E_{\gamma'}$, E_{γ} should be set to zero). Secondly, the discrete periodicity of the grating implies the conservation of the lateral momentum P_y' up to a reciprocal lattice vector, i.e.

$$\Delta P_y = n2\pi\hbar/d, \quad n = 0, \pm 1, \pm 2, \dots \quad (6)$$

For atoms this requirement can easily be derived from equation (1) if the transmission function $\tau^{\text{PP}}(P'_x, P'_y; Y)$ is assumed to have period d in its third argument. An analogous derivation can be carried out for dimers and trimers using equation (2).

Introducing polar coordinates in the xy plane, a short calculation with equations (5) and (6) shows that the n -th order principal diffraction maximum is located at [15, 17]

$$\sin \theta_n = \left(1 - \frac{E_{\gamma} - E_{\gamma'}}{P'^2/2M} \right)^{-1/2} \left[\sin \theta' + n \frac{2\pi\hbar}{P'd} \right]. \quad (7)$$

where θ_n is related to the final momentum by $P_y = P \sin \theta_n$, and the incident angle θ' is defined by $P_y' = P' \sin \theta'$. Two cases may be distinguished: for elastic ($E_{\gamma} = E_{\gamma'}$) diffraction the square root factor in equation (7) becomes unity and

the classical wave optical result is recovered. For inelastic ($E_\gamma \neq E_{\gamma'}$) molecular diffraction the zeroth order principal maximum is shifted to a larger (smaller) angle in the case of excitation (de-excitation), and the angular spacing of the diffraction maxima is increased (decreased). We note that the derivation of equation (7) involved solely the two general conservation laws (5) and (6). It applies, therefore, not only to dimers but also to larger clusters.

3 The energy spectrum of a weakly bound molecule

Molecular diffraction allows, in principal, to determine the transition energies between bound states of a weakly bound molecule. The key is to note that, according to equation (7), inelastic diffraction gives rise to additional diffraction maxima whose experimentally measurable angular spacing depends upon the transition energies $E_\gamma - E_{\gamma'}$.

To demonstrate the results presented above we consider the deuterium molecule dimer in its ortho-ortho modification, $(o\text{-D}_2)_2$. At low nozzle temperatures both constituents may be assumed to be in their lowest rotor states ($j = 0$) [17]. A dimer of two such $o\text{-D}_2$ exhibits four rotational bound states, labeled by their end-over-end rotational quantum number l . All four bound states belong to the lowest vibrational mode [18]. The interaction with the grating induces transitions between these dimer states. In the special case of equal constituents, as in $(o\text{-D}_2)_2$, however, the dimer transmission function (3) vanishes due to symmetry if the incoming (l') and outgoing (l) dimer states have opposite parity. This gives rise to the parity selection rule $l' + l = \text{even}$.

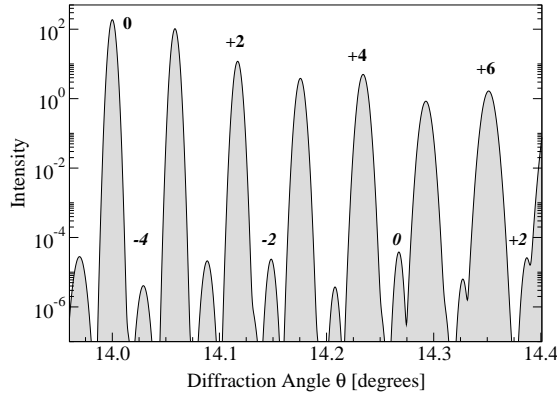


Figure 3: Calculated diffraction pattern of an $(o\text{-D}_2)_2$ beam at an angle of incidence of $\theta' = 14^\circ$. In-between the intense elastic maxima the weaker and more widely spaced inelastic maxima due to the $0 \rightarrow 2$ transition are visible. Other inelastic transitions are not resolved.

The population density of the l' -states in the incident beam may be estimated by their angular momentum degeneracy and the Boltzmann weight factors $(2l' + 1) \exp(-E_{l'}/k_B T_b)$, where the translational beam temperature is assumed to be $T_b = 400\text{mK}$ [17]. Therefore, initially only the $l' = 0$ ($E_0 = -848\mu\text{eV}$) and $l' = 1$ ($E_1 = -720\mu\text{eV}$) states are significantly populated [17]. Figure 3

shows a diffraction pattern for (o-D₂)₂ at an incident angle of $\theta' = 14^\circ$. The intense maxima are due to elastic diffraction whereas the weak maxima arise from the transition 0→2. The wider angular spacing of the latter is related to the transition energy $E_2 - E_0 \approx 377\mu\text{eV}$. Inelastic maxima of other transitions are too weak to be resolved.

4 The size of a weakly bound molecule

In this section we will review how the relative intensities in an elastic molecular diffraction pattern may be used to determine the bond length of a molecule. Starting from the transition amplitudes (1) or (2) it has been shown before [6, 9] that the n -th order diffraction maximum intensity is of the general form

$$I_n \propto \frac{\sin^2(\pi n s_{\text{eff}}/d) + \sinh^2(\pi n \delta/d)}{(\pi n/d)^2} \exp[-(2\pi n \sigma/d)^2]. \quad (8)$$

This expression contains a Kirchhoff slit function whose effective slit width s_{eff} is smaller than the geometrical slit width s of the grating. The difference accounts for the finite size of the molecule and for its van der Waals interaction with the grating. (The parameters δ and σ in equation (8) are also related to the van der Waals interaction, to irregularities of the grating, and to dimer break-up, but they will not be relevant in the following.) Generally, the effective slit width assumes the velocity dependent form

$$s_{\text{eff}}(v') = s - \text{Re} \int_{-s/2}^{s/2} dY [1 - \tau(P'_x, P'_y; Y)], \quad v' = \sqrt{P_x'^2 + P_y'^2}/M, \quad (9)$$

where τ should be replaced by the respective transmission function (cf. equations 3 and 4, and Ref. [11] for atoms). Therefore, in the case of dimers, or trimers, the full molecular bound state wave function enters into equation (9). The integration extends over one slit.

For the helium dimer, however, it was argued in Ref. [9] that the dependence on the full wave function may be neglected. Denoting the expectation value of the bond length by $\langle r \rangle = \int d^3r |\phi(\mathbf{r})|^2 r$ one obtains, after some algebra, the approximate expression

$$s_{\text{eff}}(v') \approx s - \frac{\langle r \rangle}{2} - 2 \text{Re} \int_0^{s/2} dY \left[1 - \tau_1^{\text{PP}}(Y) \tau_2^{\text{PP}}\left(Y - \frac{1}{2}\langle r \rangle\right) \right], \quad (10)$$

where the momentum arguments of the transmission functions have been omitted for better readability. Figure 4 shows helium atom (circles) and dimer (squares) data for s_{eff} , as determined by fitting equation (8) to experimental diffraction patterns. The dashed line was calculated from equation (9) for helium atoms. The solid line was calculated from equation (10) with $\langle r \rangle$ adjusted such as to obtain the best agreement with the data. A short analysis reveals that the integrals in equations (9) and (10) vanish in the limit of infinite velocity. Hence, the distance between the solid and the dashed lines in figure 4 allows to estimate the bond length to be $\frac{1}{2}\langle r \rangle \approx 2.5$ nm. A quantitative evaluation of the data yields the final result $\langle r \rangle = 5.2 \pm 0.4$ nm, making the helium dimer the largest known diatomic molecule in the ground state [9].

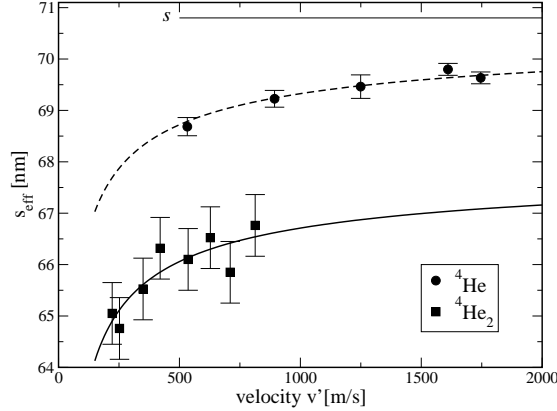


Figure 4: Experimental values for the effective slit widths of helium atoms (circles) and dimers (squares). The data were obtained by fitting equation (8) to experimental diffraction patterns measured by the Toennies group at the Max Planck Institut in Göttingen. The dashed line was calculated from equation (9). The solid line was calculated from equation (10) with $\langle r \rangle = 5.2$ nm (best fit). The thin horizontal line at the top indicates the geometrical slit width s .

For the helium trimer a similar analysis can be carried out. It follows that the effective slit width can be expressed in terms of the expectation value of the pair distance $\langle r \rangle = \int d^3r \int d^3\rho |\phi(\mathbf{r}, \boldsymbol{\rho})|^2 r$ only. In this way one obtains the approximate formula

$$s_{\text{eff}}(v') \approx s - \frac{3}{4}\langle r \rangle - 2 \operatorname{Re} \int_0^{s/2} dY \left[1 - \tau_1^{\text{PP}}(Y) \tau_2^{\text{PP}}\left(Y - \frac{1}{2}\langle r \rangle\right) \tau_3^{\text{PP}}\left(Y - \frac{5}{8}\langle r \rangle\right) \right]. \quad (11)$$

To lessen the impact of the van der Waals interaction with the grating in favor of a more accurate determination of the pair distance $\langle r \rangle$ the measurements were carried out at an incident angle of $\theta' = 18^\circ$. Therefore, the geometrical slit width s reduces to its projection perpendicular to the incident beam. The data are shown in figure 5. Analogously to the helium dimer case a comparison between equations (11) and (9) shows that the distance between the dashed line (atoms) and the solid line (trimers) is asymptotically given by $\frac{3}{4}\langle r \rangle$. A detailed quantitative analysis of the pair distance is yet underway.

5 Conclusions

A diffraction experiment setup is a sensitive measurement apparatus for weakly bound molecules. We have summarized in this article how such a setup may be employed to study two characteristic features of the bound state of a cluster: The energy level spectrum and the bond length.

In the first part we demonstrated how the energy level spectrum of a two-body cluster may be determined in a diffraction experiment by measuring the

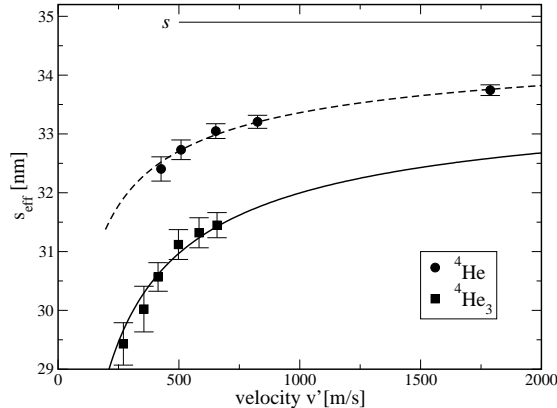


Figure 5: Experimental values for the effective slit widths of helium atoms (circles) and trimers (squares) at an incident angle of $\theta' = 18^\circ$. The solid line was calculated from equation (11) using the best fit value for $\langle r \rangle$. The thin horizontal line at the top indicates the projected slit width perpendicular to the incident beam.

angular positions of the inelastic maxima. The results were applied to the realistic example of the diffraction of $(o\text{-D}_2)_2$. The derivation of the formula (7) for the inelastic diffraction angles relies solely on two general conservation laws and is, therefore, also applicable to larger clusters [15].

In the second part we showed in which way the experimental diffraction intensities allow to determine the bond lengths of dimers and trimers. The general and intuitive concept of an effective slit width was presented, and applied to the clusters ${}^4\text{He}_2$ and ${}^4\text{He}_3$. A comparison with experimental data from the group of J.P. Toennies in Göttingen was shown. Recently, in order to determine the bond length of the helium trimer more accurately a non-zero incident angle was chosen. The analysis of this experiment is currently in progress.

References

- [1] C. Davisson and L. H. Germer, Phys. Rev. **30**, 705 (1927).
- [2] J. A. Leavitt and F. A. Bills, Am. J. Phys. **37**, 905 (1969).
- [3] D. W. Keith, M. L. Schattenburg, H. I. Smith, and D. E. Pritchard, Phys. Rev. Lett. **61**, 1580 (1988).
- [4] O. Carnal and J. Mlynek, Phys. Rev. Lett. **66**, 2689 (1991).
- [5] W. Schöllkopf and J. P. Toennies, Science **266**, 1345 (1994).
- [6] R. E. Grisenti, W. Schöllkopf, J. P. Toennies, G. C. Hegerfeldt, and T. Köhler, Phys. Rev. Lett. **83**, 1755 (1999).
- [7] R. Brühl et al., Europhys. Lett. **59**, 357 (2002).
- [8] M. S. Chapman et al., Phys. Rev. Lett. **74**, 4783 (1995).

- [9] R. E. Grisenti et al., Phys. Rev. Lett. **85**, 2284 (2000).
- [10] G. C. Hegerfeldt and T. Köhler, Phys. Rev. A **57**, 2021 (1998).
- [11] G. C. Hegerfeldt and T. Köhler, Phys. Rev. A **61**, 23606 (2000).
- [12] L. W. Bruch, W. Schöllkopf, and J. P. Toennies, J. Chem. Phys. **117**, 1544 (2002).
- [13] M. Boustimi et al., Eur. Phys. J. D **17**, 141 (2001).
- [14] M. Boustimi et al., Europhys. Lett. **56**, 644 (2001).
- [15] G. C. Hegerfeldt and T. Köhler, Phys. Rev. Lett. **84**, 3215 (2000).
- [16] B. D. Esry, C. D. Lin, and C. H. Greene, Phys. Rev. A **54**, 394 (1996).
- [17] M. Stoll and T. Köhler, J. Phys. B **35**, 4999 (2002).
- [18] G. Danby, J. Phys. B **16**, 3411 (1983).
- [19] M. Born and E. Wolf, *Principles of Optics*, Pergamon Press, 1959.